Research Article

Journal of Oil and Gas Research Reviews

Densification of the Gravity Data Using Artificial Neural Network [Ann]: Application to Structural Study of the Lom-Pangar Region [East-Cameroon]

Steve Diffo[1*], Evariste Ngatchou Heutchi[2], Marcelin Mouzong Pemi[3], Alain-Pierre K. Tokam[4], Imen Hamdi Nasr[5], Severin Nguiya[6] and Jean Marie Bienvenu Ndjaka[7]

[1]Laboratory of Geophysics and Geoexploration, Department of Physics, University of Yaoundé 1 P.O. Box 337, Yaoundé, Cameroon.

[2]Laboratory of Geophysics and Geoexploration, Department of Physics, University of Yaoundé 1 P.O. Box 337, Yaoundé, Cameroon.

[2]Department of physics, Advanced Teacher Training College, University of Yaoundé 1 P.O. Box 47, Yaoundé, Cameroon.

[3]Department of Renewable Energy, Higher Technical Teachers' Training College (HTTTC), University of Buea, P.O. Box 249, Buea Cameroon.

[4]Laboratory of Geophysics and Geoexploration, Department of Physics, University of Yaoundé 1 P.O. Box 337, Yaoundé, Cameroon.

[5]Laboratory of Geophysics Faculty of Sciences of Bizerte, Tunisia (FSB Tunisia) 7021 Jarzouna, Bizerte, Tunisia.

[6]National Advanced School of Engineering, University of Douala, P.O. Box 2701, Douala, Cameroon.

[7]Laboratory of Mechanics, materials and structures Department of Physics, University of Yaoundé 1 P.O. Box 337, Yaoundé, Cameroon.

***Corresponding Author**
Stève Diffo, Laboratory of Geophysics and Geoexploration, Department of Physics, University of Yaoundé 1 P.O. Box 337, Yaoundé, Cameroon.

Submitted: 2023, Oct 24; **Accepted:** 2023, Nov 14; **Published:** 2023, Nov 17

Citation: Diffo, S., Heutchi, E. N., Pemi, M. M., Tokam, A. P. K., Nasr, I. H., et al. (2023). Densification of the Gravity Data Using Artificial Neural Network [Ann]: Application to Structural Study of the Lom-Pangar Region [East-Cameroon]. *J Oil Gas Res Rev, 3*(2), 101-118.

Abstract

For better understanding of the Lom-Pangar structural settings, a gravity field study was carried out. This area is intermediate between the Congo Craton [CC] in the south and the Pan-African in the north. Also, it is an active tectonics zone evidenced by the geological complexity and some shearings that gave rise to numerous major faults [Sanaga Shear Zone and the Central Cameroon Shear Zone] crossing this region. Although it is a high potential mining, zone very few gravimetric studies have been conducted probably due to the poor coverage of available Bouguer anomaly data. There is therefore a necessity to performed very high-resolution interpolation to be able to figure out the real tectonic settings. This pioneering work on the artificial neural network applied to these gravity data has improved the gravimetric coverage of the Lom-Pangar region to a resolution: of 2.90 arc minutes].

The findings from the densified gravity data using the artificial neural method reveal many deeply rooted structural features oriented along the NE-SW, NW-SE, and ENE-WSW directions in this region. The ENE-WSW trend is strongly developed than the other identified trends correlating with the main shear zones crossing the region. The good clustering observed on the local maxima of the horizontal gradient magnitude of the vertical drift and the Euler solutions suggests that the delineated contacts have vertical dips [faults of vertical extension up to 20km], to subvertical [contact boundaries materializing sedimentary basins or gravity domes preceding a dense material intrusion phenomenon]. As

the basement of the region is granite-gneissic, migmatites and gneisses ensure the faulted contacts in the region. Newly identified faults are considered as strike slip with lateral and vertical extensions of the Sanaga Shear Zone or the Central Cameroon Shear Zone. These new identified features are evidences of the strong geodynamics activities taking place in the study area.

Keywords: Gravity Data, Artificial Neural Network, Lineaments, Filtering, Multi-Scale Analysis.

1. Introduction

In recent decades, several geophysical works have been in the area carried out by scientists. such as with their studies on at the pan-African and Gondwana level have improved the knowledge of the geology of Cameroon [1]. The general view of the geology of the study area have been provided by a compilation of data from the explanatory note on the Batouri-Est sheet presented by [2-4]. The high degree of isolation has long tile hindered the geophysical investigation in the Lom-Pangar region despite the fact that it is a high potential mining area. This results in low and very sparse gravity data coverage, impacting therefore the quality of geophysical results in the region [5].

However, previous geological and geophysical studies show that the East Cameroon region has real mining potential [6]. For this reason, there is a necessity to improve the gravity data coverage in this region before any analysis could be conducted, either by carrying out new geophysical survey campaigns, which appears costly or by using an efficient interpolation method. Considered the neural methods as an interpolation technique for Bouguer anomalies [5]. In addition, the gravimetric method based on the difference in gravity of the actual subsurface structures compared to the density obtained, proves to be particularly effective when characterizing the structural architecture in the area. Indeed, based on density differences, it indicates some important structural features that cannot be followed with morphotectonic tools.

Given the importance of linear anomalies in geophysical characterisation, special attention be given to the strong contrasts [gradients] present in the transformed Bouguer anomaly maps, in order to detect discontinuities such as flexures, dykes and faults. In the present study, two methods are combined: The neural method that improves the gravimetric coverage of the study area; then the gravimetric method which will is a comparative analysis of the Bouguer map from in-situ data compared to the one from the neural method [ANN]. An analysis of the vertical derivative of the horizontal gradient maps coupled with that of the upward continuation methods and the Euler-3D solutions have been conducted. Finally, the aim of this work is to use a multiscale analysis coupled with Euler-3D deconvolution of densified gravity data following the artificial neural network, to accurately map lineaments in the Lom-Pangar region.

1.2. Geological Context

The study area covers from north to south the parallel 4˚30'N, and 6˚10'N, and from the west to east the meridian 11˚30'E and 13˚45'E [Figure 1]. It covers three regions of Cameroon, including parts of the East, Centre, and Adamaoua. A synthesis of previous studies testify that Central Africa is mainly made up of granitic rocks and metamorphic rocks, which outcrop from Cameroon to Sudan [7-12]. These rocks belong to various eras and are outcrops. They are mainly granites and migmatites rejuvenated during the Pan-African episode. The geological history of East Cameroon ranges from the Archean to the present day, with litho-stratigraphic formations and tectonometamorphic events.

Concerning the Pan-African chain in the Eastern region of Cameroon, studies conducted by highlight the Central African Orogenic Belt [CAOB] in the region, which stretches for nearly 4000 km, and hosts the Tchollire-Banyo Shear Zone [TBSZ], the Central Cameroon Shear Zone [CCSZ], and the Sanaga Shear Zone [SSZ] further north. The first [CCSZ], crosses the NW region of the study area with an oblique crossing of the Adamawa Plateau [13, 14]. The first [SSZ] is located to the south of Lom-Pangar in the central region and the second one in the SW region of the map [Figure 1]. These shears above mention features highlight a mylonitic fabric that would have developed differently at the level of the igneous granitic intrusions but also within the metamorphic gneisses and migmatites.

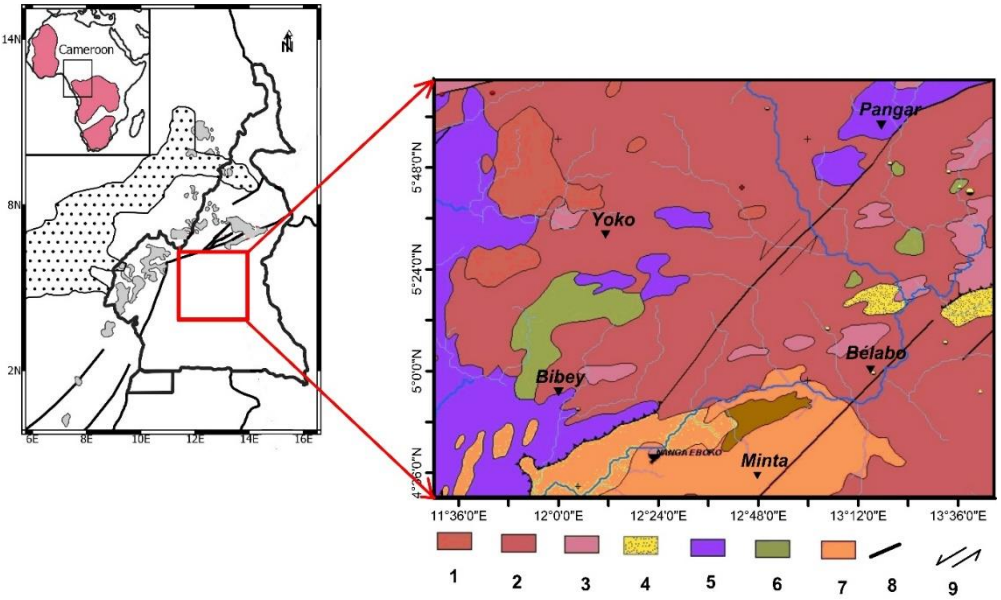

1: Post-tectonic granitoids; 2: Syn to late-tectonic granitoids; 3: Pre- to syn-tectonic granitoids; 4: Sedimentary schist; 5: Granitic gneisses; 6: Detrital sediments; 7: Gneisses and micaschists; 8: Faults and 9: Fault movement

Figure 1: Geological Map of the Study Area [[5]; modified].

The geological map of Cameroon derived from figure 1 highlights three main formations: magmatic formations, Precambrian metamorphic formations, and non-metamorphic sedimentary formations. These formations are located in the mobile zone of Central Africa, which covers almost two-thirds of Cameroon's territory, and have been affected by the tectonic events that have damaged the central part of the old continent, particularly Cameroon, and are favored areas for mining deposits [15].

2. Data and Methodology

The gravity data used in this study have been collected by the British geophysical company GETECH Group plc, for Central and West Africa. They were obtained after compiling all the gravity surveys carried out in Cameroon and neighboring countries by various organizations and researchers between 1959 and 1985. Figure 2 shows the position of the gravity stations, which are spaced between 3 and 10 km and more apart. The data distribution is approximately 220 stations per square degree. The location of the stations was determined on topographic maps and by compass bearings.

The error in the position of the stations is about 200 m. Gravity measurements were made using various gravity meters: Lacoste & Romberg [Model G, Nos. 471 and 823], Worden [Nos. 69, 135, 313, 600, and 1153], World Wide [No. 36], Canadian Scintrex [No. 305G] and North-American [Nos. 124 and 165]. Corrections were made to the readings taken with the gravimeter and the gravity anomalies were calculated in relation to an average crustal density of 2.67 g/cm3; i.e. the accuracy of the gravity values is of the order of 0.2 mGal. The measurements were related to the reference stations known as the gravimetric bases of the Martin network.

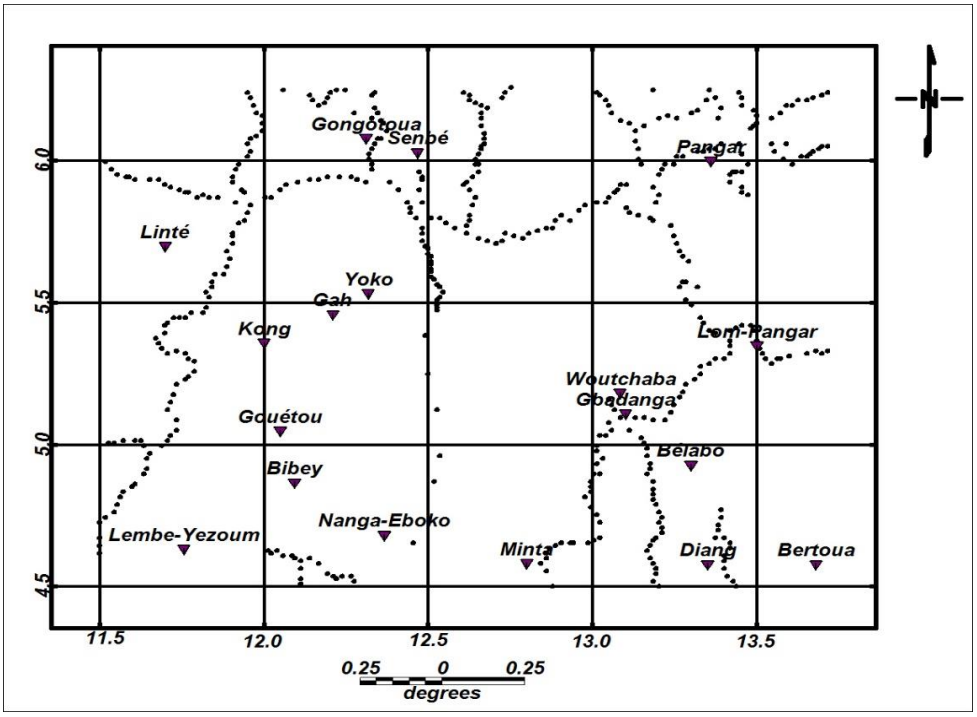

Figure 2: Distribution Map of the In-Situ Measurement Points of the Gravimetric Data

Figure 3 represents the Bouguer anomaly map obtained from in-situ data. It is calculated by compiling gravity data from 466 measuring stations irregularly distributed over the study area; using an interpolation program, a Bouguer anomaly map was generated.

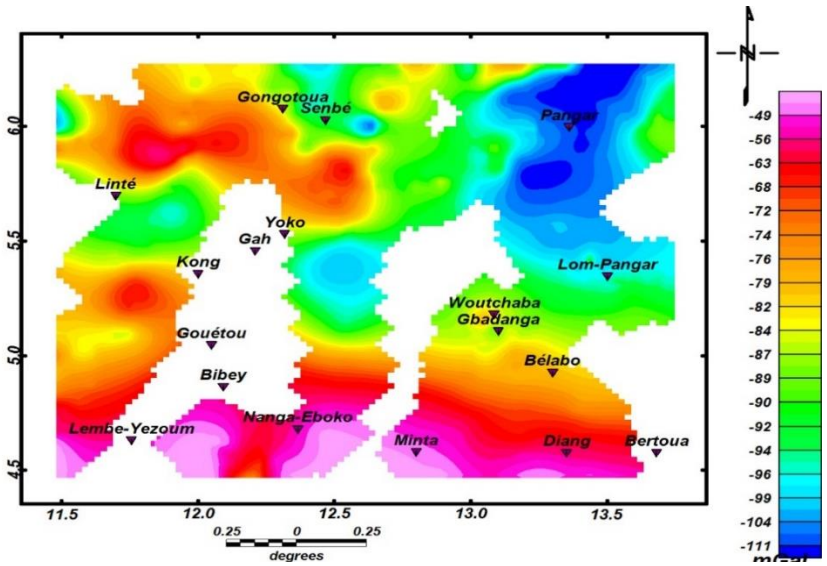

Figure 3: Non-Interpolated Bouguer Anomaly Map of the Study Area

In fact, the study area with more than 47400 km2 122 has a data distributed over a resolution less than 0.01 data per km2 123. This is very insufficient for an efficient structural study. It is therefore important to conduct another field trip in order to collect more data [which is very expensive] or to apply an interpolation technique capable of filling these "gaps" as well as guaranteeing certain geostatistical reliability. Due to the latest advances of the neural method in geosciences, it will therefore be used to obtain a better Bouger anomaly map.

The main goal of this work is to densify the in-situ gravity data of the Lom-Pangar region using the neural method [ANN], in order to carry out a structural study based on a multiscale analysis coupled with Euler-3D deconvolution. This combination of techniques has the particularity of highlighting the gravity signatures of geological features in the subsurface [16].

2.1. Artificial Neural Network Method

As this study is a continuation of the one carried out by, which

gives all the literature associated with the neural method as well as the Levenberg-Marquardt multi-layer perceptron back propagation algorithm. The design and implementation of the artificial neural model consider the following steps [5].

2.2. Data Collection and Pre-Processing

From a total of 466 samples obtained for this test region, 60% [i.e. 280] were used for the computation with the multilayer perceptron network, 20% [i.e. 93] for network testing and the remaining 20% for the validation test. The problem of missing data and normalization is solved immediately after data collection through the pre-processing procedure. First, the missing data is replaced by the average of the neighboring anomaly values surrounding that area. The normalization procedure is strongly recommended as the learning algorithm will tend to confuse small variables with large ones as they are all mixed together; the algorithm will react by rejecting variables of smaller magnitudes at the expense of larger ones. The Bouguer anomaly values have been normalized to the interval [-1,1] using the following relationship (1):

$$B_{nor} = \frac{2(B - B_{min})}{B_{max} - B_{min}} - 1 \qquad (1)$$

At the end, the anomaly values are de-normalised using equation (2)

$$B = \frac{1}{2}(B_{nor} + 1)(B_{max} - B_{min}) + B_{min} \qquad (2)$$

2.3. Network Construction

The connection weights/biases are iteratively adjusted during the learning process, in order to minimise the deviation between the predicted output [following the ANN] and the actual output [Bouguer anomaly measured in-situ]. Several combinations of transfer functions and different network models are to be considered in order to find the best architecture for which the correlation is very high, the mean squared and bias errors as low as possible. Figure 4.a) presents a simplified example of a multi-layer perceptron architecture model applied in this study. MatLab provides transfer functions embedded in the artificial neural network processing routine, which are used in this study. The Levenberg Marquardt learning algorithm was used, which is a back-propagation algorithm for training the neural network. Figure 4.b) shows one of the possible architectures of the network generated from the MatLab software during the implementation with two inputs, a hidden layer with 15 neurons, ending with an output.

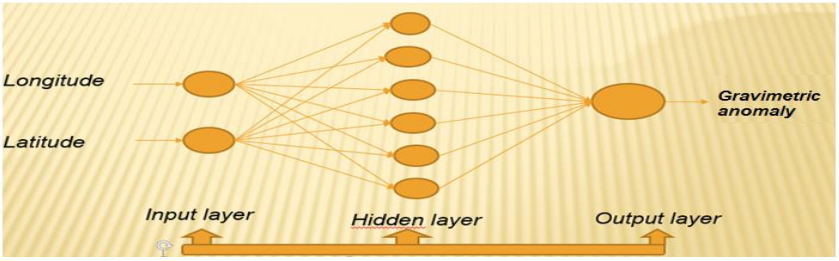

Figure 4.a): Multi-Layer Perceptron Network

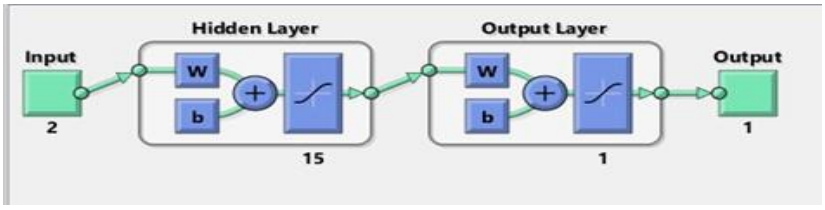

Figure 4b): Architecture of the Neural Network

2.4. Testing the Network

The aim here is to test the performance of the developed neural model. For the Lom-Pangar region, 93 samples of in-situ gravity data were used to conduct this operation. The statistical evaluation of the performance of the developed artificial neural model consists in evaluating some parameters such as the correlation coefficient [R2], the Root Mean Square Error [RMSE] or the Mean Bias Error [MBE]. The correlation coefficient gives the degree of similarity between the original Bouguer anomaly values and those generated by the artificial neural network. The closer this value is to 1 [or 100%], the better the artificial neural network model generated is considered to be suitable for the study. Extended to a small scale, the root mean square error provides information about the performance of the artificial neural network. It measures the variation of the predictive values with respect to the measured data.

In contrast to the correlation coefficient, the lower it is, the more accurate the estimate. The evaluation of the performance of the neural model to be extended to a large scale is made possible through the mean bias error. It specifies the average deviation between the predicted values and the original ones. Expressions (3), (4) and (5) calculate the mean square error, mean bias error, and correlation coefficient respectively.

$$RMSE = \sqrt{\frac{1}{n}\sum_{i=1}^{n}(B_{p,i} - B_i)^2} \quad (3)$$

$$MBE = \frac{1}{n}\sum_{i=1}^{n}(B_{p,i} - B_i) \quad (4)$$

$$R^2 = \frac{\sum_{i=1}^{n}(B_{p,i} - \bar{B})^2}{\sum_{i=1}^{n}(B_i - \bar{B})^2} \quad (5)$$

2.5. Gravimetric Method

The analytical processing tools used in this study are the upward extension [UC] and horizontal gradient vertical derivative [HGDV] methods and Euler-3D deconvolution in order to estimate the depth of the identified lineament structures. This study applies the horizontal gradient vertical derivative technique to continuous upward gravity grids at different heights in order to evaluate the peaks in the involved grids. The technique is called multiscale analysis [17]. It consists of: first, establish the 1st 188 order vertical derivative map of Bouguer anomalies at different heights.

Then, on each map obtained, apply the horizontal derivative filter and determine the local maxima/minima. And finally, superimpose the local maxima/minima obtained on the different maps on a single map. The degree of importance [in depth] of a fault and or lithological contact is determined by the persistence of the presence of local maxima for higher and higher extension altitudes. The same criterion allows a qualitative comparison of the relative depths of the intrusive bodies; moreover, the displacement of the maxima could allow determining the direction of inclination of the highlighted contacts.

3. Results

3.1. Densified Gravity Map

The neural network is designed by introducing into the system the inputs [longitude, latitude], and the system parameters such as the number of hidden layers, the number of neurons in each layer, and the transfer function [linear [pureline], hyperbolic sigmoidal tangent [tansig] and sigmoidal logarithm [logsig]]. During the learning process, the connection weights/biases are adjusted to make the predicted outputs close to the actual outputs [Bouguer anomaly]. During the implementation, several architectures are generated by varying the parameters of the neural architecture mentioned above; for each architecture generated, statistical quantities such as MBE [Mean Bias Error], RMSE [Root Mean Square Error] and the Correlation Coefficient are calculated according to the output obtained.

This section presents the results obtained from the multilayer perceptron model of the artificial neural network.

Table 1 shows the computed statistical parameters [R2 207, RMSE, MBE] considering 15 different network architectures. It highlights the performance of the generated neural network according to the chosen architecture.

Model	Transfert function	inputs	Structure of the network	R^2	RMSE	MBE
1	linear	Long itud	2-6-1	0,8580	0,8571	-0,1532
2			2-10-1	0,8581	0,8500	0,0761
3			2-15-1	0,8258	0,8634	-0,1472
4			2-17-1	0,8479	0,8740	-0,1405
5			2-20-1	0,8876	0,8563	0,1161

6	Hyperbolic sigmoidal tangent	longitude and latitude	2-6-1	0,9223	0,1609	0,0080
7			2-10-1	0,9547	0,1238	0,0037
8			2-15-1	0,9750	0,0923	-2,34E-6
9			2-17-1	0,9715	0,0986	0,0032
10			2-20-1	0,9811	0,0804	0,0003
11	Sigmoidal logarithm	longitude and latitude	2-6-1	0,9180	0,8655	0,0561
12			2-10-1	0,9277	0,2450	-0,2837
13			2-15-1	0,9493	0,0915	0,0313
14			2-17-1	0,9263	0,2315	0,1418
15			2-20-1	0,9541	0,3314	0,0088

Table 1: Input and Statistical Error Parameters of Models Developed for Different Neural Network Architectures.

From the previous investigation of conducted in the Lom-Pangar region, it appears that the neural architecture capable of densifying the Bouguer anomalies in the study area contains 20 neurons in the hidden layer and uses the sigmoidal tangent function as a transfer function. Indeed, its statistical parameters are as good as possible [R2=0.9811; RMSE =0.0804; MBE =0.0003] [5].

Figures 5 present the new distribution of the measurement points where the Bouguer anomaly data have been estimated. The validation of the neural architecture from a gravimetric point of view will be done following a comparative analysis on figures 6, 7 and 8 which correspond respectively to the Bouguer anomaly maps, the upward continued maps and the derived maps.

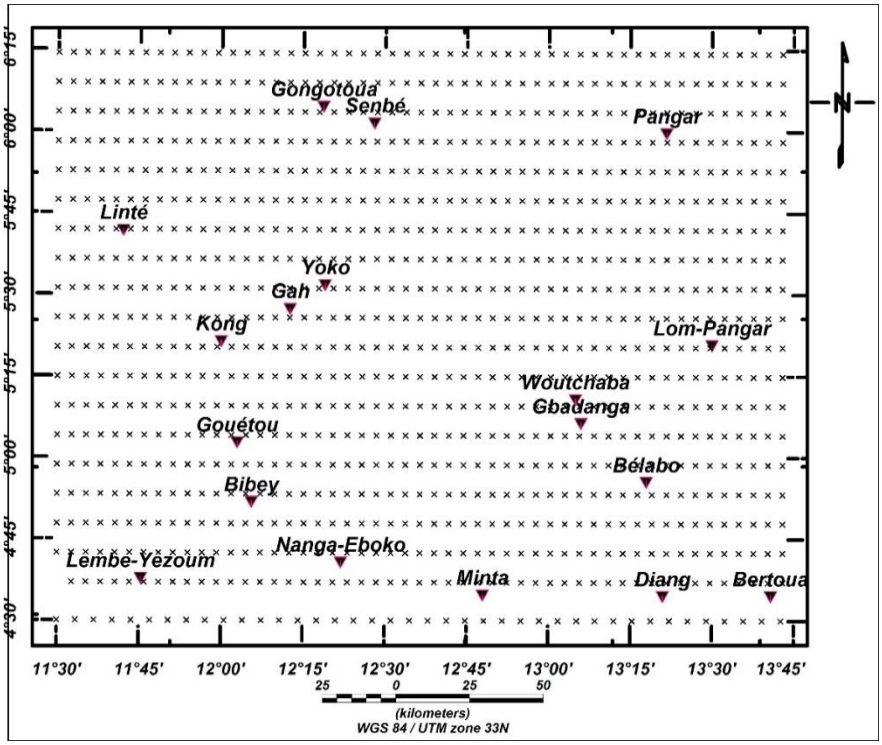

Figure 5: New Distribution Map of Estimated Gravity Data Points Following the Neural Approach

3.2. New Bouguer Map Densified by the Neural Method

Starting with 466 data points scattered over a study area of about 47400km2 222, the neural network selected will be used to densify them up to 920 Bouguer anomaly values with a regular grid [resolution] of 2.90 arc minutes. The new Bouguer anomaly grid will then be generated from this current grid. Figure 6.a) shows the Bouguer anomaly map of the in-situ data while Figure 6.b) is the new Bouguer anomaly map generated from the densified data following ANN. The specificity of the neural method will also be discussed based on the geological and tectonic information that these areas would reveal. Some disparities between the Bouguer model generated by ANN and the one obtained from in-situ data. The main areas of disparity are those not surveyed during the gravity campaign. In these areas, the mesh was made by interpolation following the minimum curvature [figure 6.a] or by ANN [figure 6.b].

The strong negative anomalies on the south of the Lom-Pangar locality in Figure 6.b) could be evidence of the extension of the Lom sedimentary basin within the study area, and correspond to the sedimentary deposit identified on the geological map [Figure 1]. The limitation restrictin of the positive extension to the NW of the study area in favor of a very slight anomaly would constitute, due to this difference in anomaly direction N 42° E, information on a probable contact or fault zone. These two hypotheses would be strongly considered because the CCSZ fault is identified on the geological map in this area and the Post-tectonic granitoids, Syn to late-tectonic granitoids and Granitic gneisses formations overlap. These elements attest that the neural model is a better interpolator of the Bouguer anomaly data.

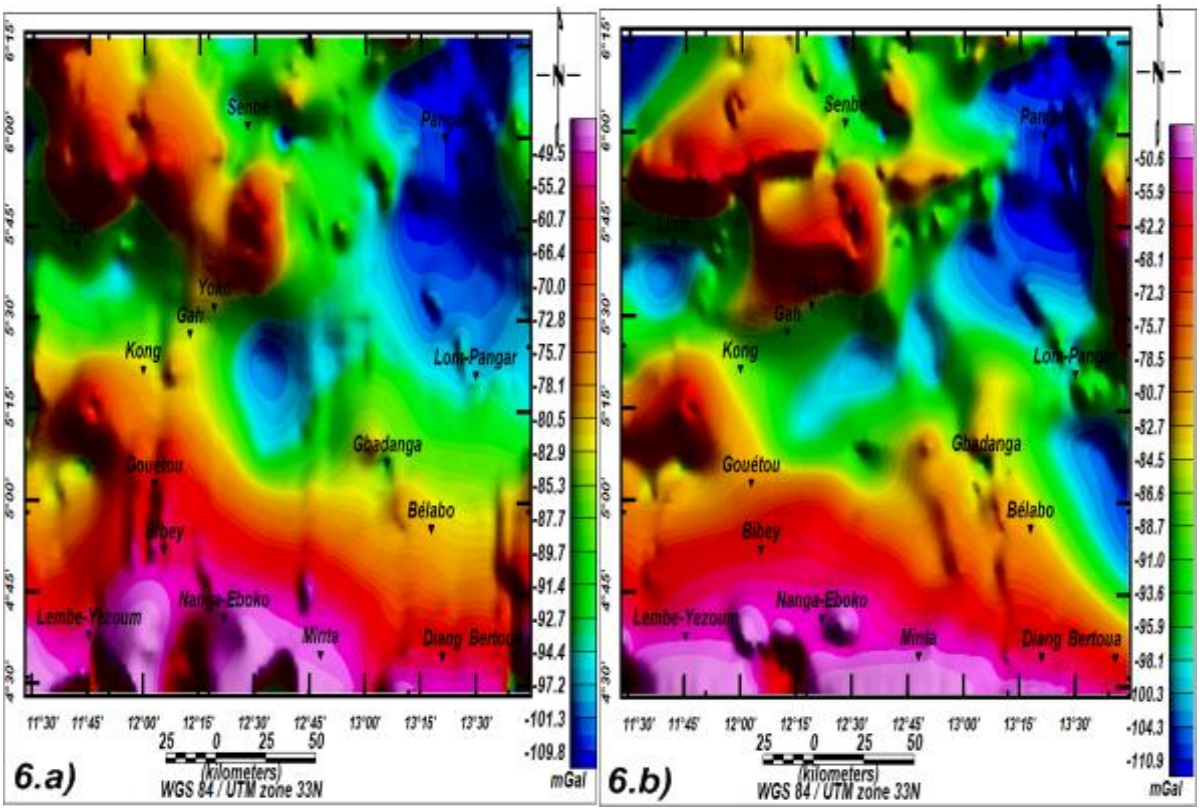

Figure 6: Bouguer Map of the Lom-Pangar Region [6.a In-Situ Data; 6.b ANN Data]

Firstly, in the far south and NW of the region, there are strong anomalies with values between -77 mGal and -51 mGal; considering their more or less spherical or cone-shaped three-dimensional anomalies characteristic of domes, an intrusion of dense rocks could be suspected, or an upwelling of dense material from the depths in the NW and the South. The second zone is the central part characterized by medium anomalies [-94 mGal to -77 mGal]; intermediate compared to strong and light anomalies. This can be seen in the localities of Sembé, Gah, Linté, Wountchaba, Lom-Pangar, etc. At the end, to the NE and then to the South of Yoko, there are very light anomalies [-94 mGal to - 112 mGal], with closed isogal curves.

They roughly draw ellipses characteristic of three248 dimensional anomalies in the form of basins or clusters, but also characteristic of cylindrical structures such as synforms, antiforms, veins, or galleries. These different structures have previously been highlighted by [18-20]. The gravity anomalies of the Lom sedimentary basin, cover both gneissic formations and huge granitic outcrops, sometimes embedded by sediments and volcanic outcrops. When compared to the geology of the region, several hypotheses can be put forward to justify the presence of different formations. The negative anomaly could be due to a schistose band that would extend and thicken under the essentially granite-gneissic nappes, or it could be due to the effect or under the effect of the isostatic compensation set up by a sinking

[the root] of the crust in the heavier upper mantle. The second hypothesis seems to be closer to reality thanks to the comparison of Bouguer's map with the geological map.

Indeed, seismological studies reveal a normal crustal thickness [33km] to the south of the Adamaoua Plateau [Lom-Pangar region], and less than so [23 km] northwards. The southern area of the map, which is characteristic of the strong positive anomalies, should be evidence of uplift of the Pan-African basement, which would be responsible for almost all the positive gravity anomalies in the area. The effects of a plate suture would be a consequence of an alignment of these positive anomalies [19, 21-24]. It could thus represent the boundary between the Adamaoua and South Cameroon massifs, characterized by metamorphic formations and a series of granitic plutons showing intense magmatic activity. The gradient zone observed to the north of Linté is probably the trace of the Central Cameroon Shear Zone [CCSZ].

These results agree with those obtained by and suggesting a lithospheric thinning under the Adamaoua Plateau, follows by a lighter asthenospheric uplift of about 40 km. In the south of the map, a very high lateral gradient is observed, with W-E direction isoanomals around the 5°N parallel in which the localities of Gouétou and Bélabo are located. This gradient evolves around Kong and Yoko with a NE-SW direction [25]. It separates the positive gravity sector to the south from the negative sector, and thus denotes a major tectonic structure penetrating the crust. This structure seems to mark the transition from the northern to the southern domain. The gradient located to the NW of Pangar and passing through Gongotoua seems to denote the northern limit of the Mbéré Gap.

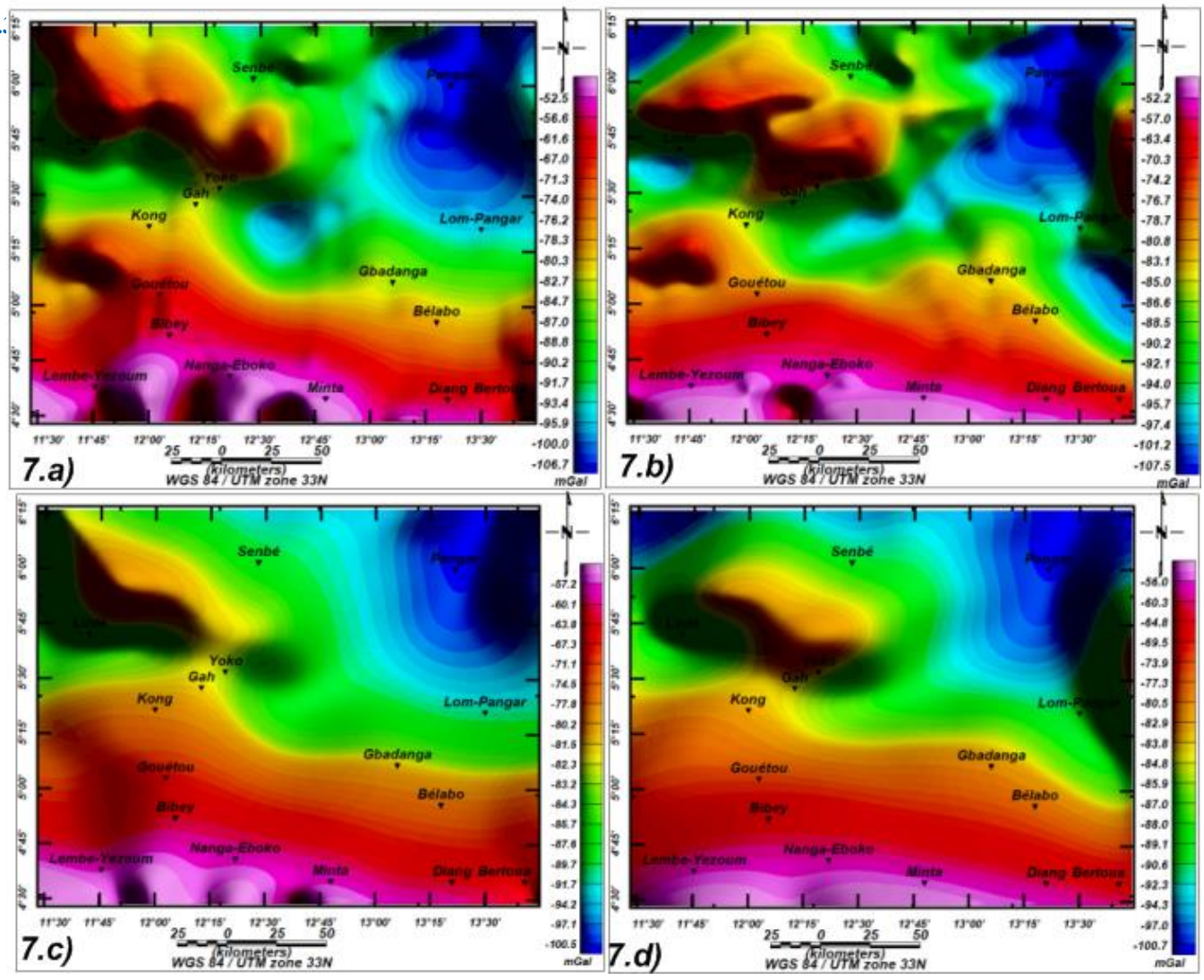

Figure 7: Upwards Continued Map at 4km [7.a In-Situ Data; 7.b ANN Data] and 20 km [7.c In-Situ Data; 277 7.d ANN Data]

This operation accentuates on the one hand the effect of deep gravity sources and attenuates or even suppresses on the other hand the influence of surface sources [26]. This low-pass filter transforms and smoothes the uneven Bouguer anomalies into smoothed anomalies, thus highlighting the regional crustal characteristics according to depth. Figure 7 compares the 4 and 20 km up warded maps obtained from the non-densified data [Figure 7.a and 7.c] and the one obtained from the ANN after the data have been densified [Figure 7.b and 7.d]. From the amplitude of the anomalies, the original Bouguer as well as the den-

sified one present are almost the same; that is to say 60,3 mGal. However, this difference in amplitude increases progressively as the amplitude of the extension increases.

At 4 km it goes from 54.2 mGal [Bouguer In-situ] to 55.3 mGal [Bouguer derived from ANN], giving a difference in amplitude of 1.1 mGal. At 20km the anomaly amplitude increases from 43.3 mGal [Bouguer In-situ] to 44.7 mGal [Bouguer derived from ANN], making a difference in amplitude of 1.4 mGal. These elements prove a better coverage of gravity data on the densified Bouguer maps using ANN. The surface and individual anomalies are levelled in proportion to the altitude of the upward continuation. The regional structure of the study area is seen through the persistence of the negative anomalies around the Pangar locality [Fig.7, d]. This NNE-SSW regional structure corresponds to the orientation of the negative anomalies in the region [27, 20].

The strong anomaly zones [both positive and negative] appear to a lesser extent marked respectively in the South and NE where an extension of the latter towards the West. The highly pronounced positive anomaly formations in the south of the study area remain clearly visible as those of the negative anomaly at Pangar. However, the negative anomalies south of Linté and Yoko tend to disappear completely, reflecting the presence of sedimentary basins located at the depth of less than 4km. The isoanomal curves become progressively linear with a major WNW-ESE direction crossing the localities of Yoko, Kong, and Wountchaba. The gravimetric structure is progressively seen at the regional level.

3.4. Gravity gradients

Vertical derivative and horizontal discontinuities: Figures 8.a) and 8.b) show the vertical derivative maps of the Bouguer anomalies of the in-situ and densified data respectively. It is noted that while the minimum is the same for both maps, the maximum is much higher for the map of the horizontal derivative densified using the ANN method [from 1.4 mGal/km to 2.1m Gal/km]. This increased amplitude associated with the good distribution of the data makes it easier and more interesting to use the vertical derivative map in the determination of horizontal contacts.

The vertical derivative highlights horizontal contacts between geological structures of different densities in the soil/subsoil with depth along z. On this map, there are vertical gradients of anomalies with values ranging from - 1.7 to 2.1 mGal/km, i.e. an amplitude of about 3.8 mGal/km. The Lembé-Yézoum, Bibey, Gouétou, and Minta anomalies stand out and are characterised by a positive gradient that peaks up to 1.5 mGal/km and has a common NWW-SEE direction. Gross gravity anomaly contrasts highlight a gradient zone similar to the Sanaga Shear Zone [SSZ] [28].

Zones north of Linté with a strong positive gradient, WSW-ENE direction, and curvilinear shape are framed by negative anomaly zones, clearly highlighting structural features in this area that coincide with the Central Cameroon Shear Zone [CCSZ] [14]. The Kong, Gah, and Yoko zones line up perfectly with a gradient line that could be either the edge of a cavity or a lineament that could be materialized by a fault. These anomalies seem to form a rectilinear and continuous network of geological contacts with lineaments that are visibly linked to faulted structures buried in the ground. These anomalies are probably related to subsurface sources.

Horizontal Gradient and Lateral Discontinuities: The horizontal derivative maps of the initial and densified Bouguer anomalies are shown respectively in figures 8.c and 8.d. It can be noticed that the minimum value appears to be the same for both maps; however, the maximum is much higher for the map of the horizontal derivative densified by ANN [from 1.7 mGal/km to 2.2m Gal/km]. This increased in amplitude, associated with the good distribution of the data allow to easily use the horizontal derivative map in determining lithological contacts and tectonic signatures.

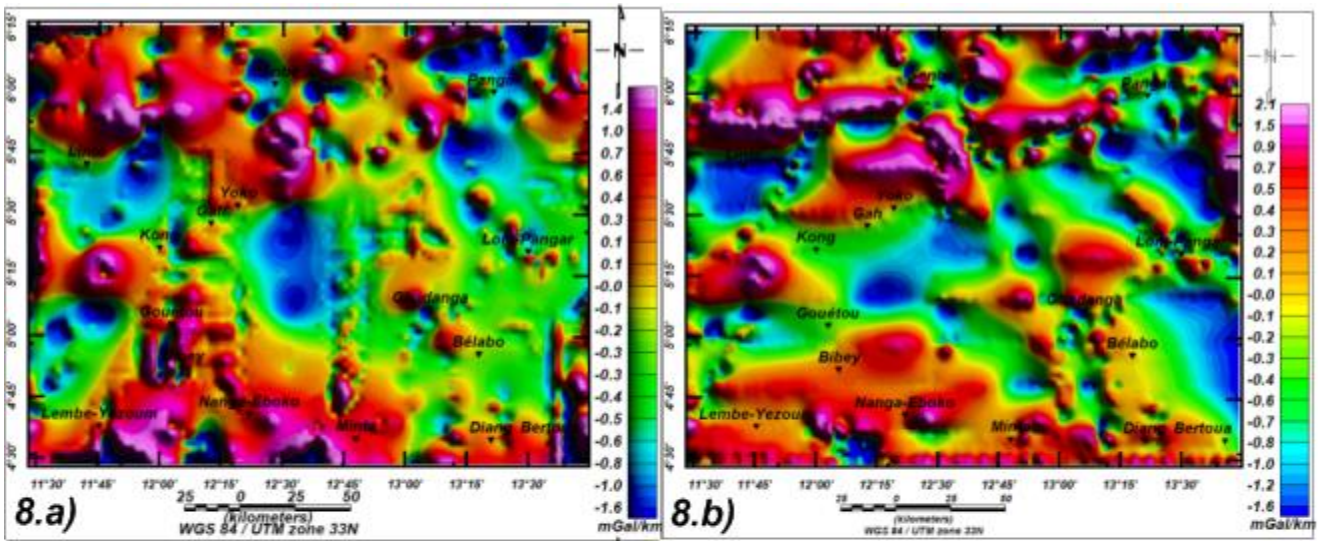

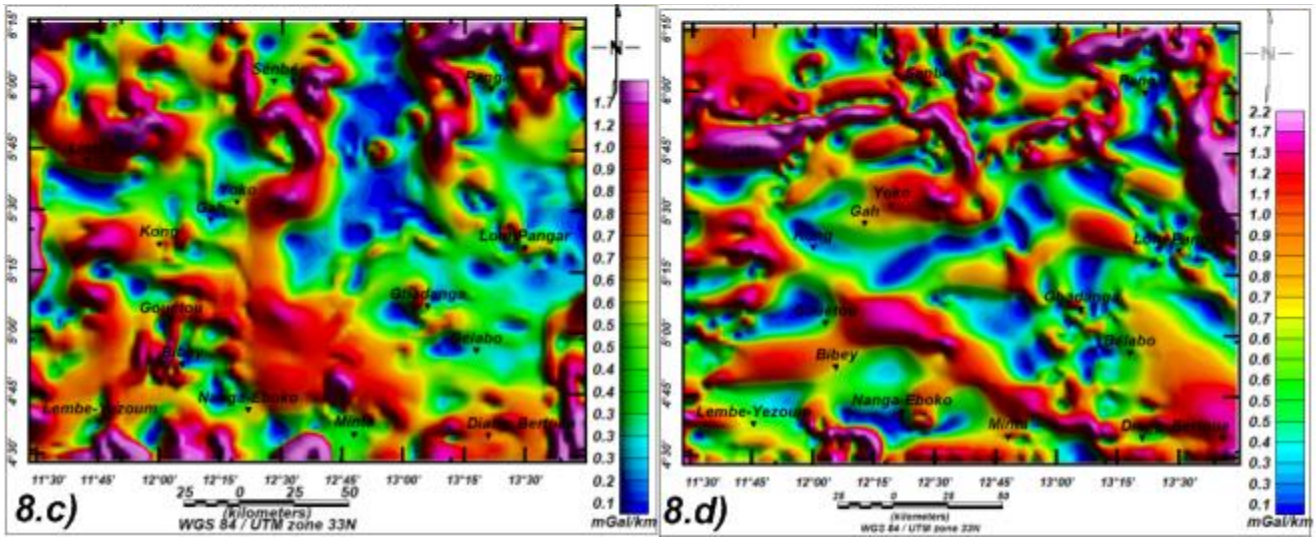

Figure 8: Vertical [8.a In-Situ Data; 8.b ANN data] and Horizontal [8.c In-Situ Data; 8.d ANN Data] Derivative Maps

The Horizontal Derivative Map is the most straightforward approach to locating lateral geological contacts between bodies of different densities in the soil/subsoil. The HD map [Figure. 8b] of Bouguer gravity data densified by the neural method, suggests that the basement of the Lom-Pangar region is generally subject to tectonic activity, insofar as zones of strong gradients are present throughout the study area, it is assumed that strong HD amplitudes will be globally correlated with faults or contacts [29, 30]. It is also noted that the gradient zones are more visible and sharply contoured with amplitude between 0 and 2.2 mGal/km. This map also suggests that the localities: West of Gouétou, Kong, Nanga-Eboko and following a SW337 NE direction as being the most stable of the crust. The localities from south of Gah to Pangar are also found to have domains with very low amplitude gradients.

South of Gongotoua, around the localities of Gah, Pangar, and passing through Linté, the presence of significant horizontal gradients [≥ 2mGal/km] is observed, which contours are circular, and follow the W-E and NEN-SWS directions. Depending on their shape, they are associated with faults and subvertical geological contacts. East of Gouétou, NE of Lom-Pangar, north of Linté and Bertoua, there are high amplitude gradient zones with more or less curved shapes; the ridge roughly draws a rounded contour revealing the presence of a subsurface igneous intrusion, dome, or diapir; which corroborates with the geological map of [4]. The horizontal and vertical gradient gravity maps [Figure 8] suggest an area strongly influenced by relatively intense tectonic activity affecting its subsurface.

The presence of tectonic activity is marked by the presence of high elongated gradients that may be associated with fractures or faults on the one hand; on the other hand, high amplitude anomalies with close contours could be due to the intrusions. Then, to the south and northwest, elongated anomalies with strong gravity gradients are correlated with the uplift of mantle materials, or could correspond to faults, fractures or contacts zones. The relatively low gradient values shown on the densified Bouguer gradient maps may characterise the presence of low-density crustal structures.

Horizontal Gradient Maxima of the Vertical Derivative [HGMVD] Coupled with an Upward Continuation: The horizontal gradient maxima of the vertical derivative of the Bouguer anomalies shown in Figure 8 identify the areas where abrupt density variations are noted. Multiscale analysis of these maxima from Bouguer maps upwards at different altitudes characterises the vertical extension of anomalous structures. The linear arrangement of many maxima provides information on the presence of faults, while quasi-linear or quasi-circular maxima indicate the horizontal limits of contacts or intrusive bodies [31, 17]. The map obtained from the superposition of HGVD maxima calculated following the Bouguer densified by the neural method extended upwards from 0 to 20 km with a constant step of 4 km, is represented on figure 9.

The exploitation of the horizontal and vertical gradient maps extended to different altitudes allows to generate directly the maxima for different depths. By superimposing these maxima, the lateral and vertical extensions of the structural signatures could be characterised. Figure 9 highlights different shapes resulting from the alignment of the maxima. Indeed, the quasi-linear or circular gradients witness the density variations within the crust in the Lom-Pangar area, which can be associated with contacts [circular shape] or faults [quasi-linear shape]. In the end, a succession of linear maxima [HDVD] are indicative of the presence of lineaments that can be interpreted as faults or contacts identifiable in the study area, as suggested by [27, 32, 33].

The alignment of the maxima follows the orientation of the main gradient zones recorded above; it also highlights the presence and vertical extension of the main faults crossing the study area [CCSZ and SSZ]. The presence of maxima at different depths [0, 4, 8, 12, 16, and 20 km] testifies to the fact that the Lom-Pangar region like the greater southern Adamaoua region has undergone considerable tectonic activity. The sedimentary zones show very few lineaments, particularly in the basin south of Linté, Gah

and Pangar. The alignment of these lineaments is evidence of the lineamentary structures which can represent gravimetric discontinuities;

They are materialized either as fractures with or without collapse of the basement [this is the case for those crossing the northern localities of Linté in a WSW-ENE direction or to the west of Lembé-Yezoum] or as cavities corresponding to intrusions of less dense bodies or, on the other hand, to the upwelling of denser bodies [the one surrounded by the localities of Linté, Gongotoum, and Pangar], Linté, Gongotoua, and Yoko] certainly occurred as a result of intense tectonic activities. These intense discontinuities NWW-SEE and NEE-SWW would probably mark extensions of the limits of the Lom Basin, to which the Lom-Pangar region belongs. These indicators support the hypothesis of a common tectonic history between the Lom Basin and the Mbéré Gap [27].

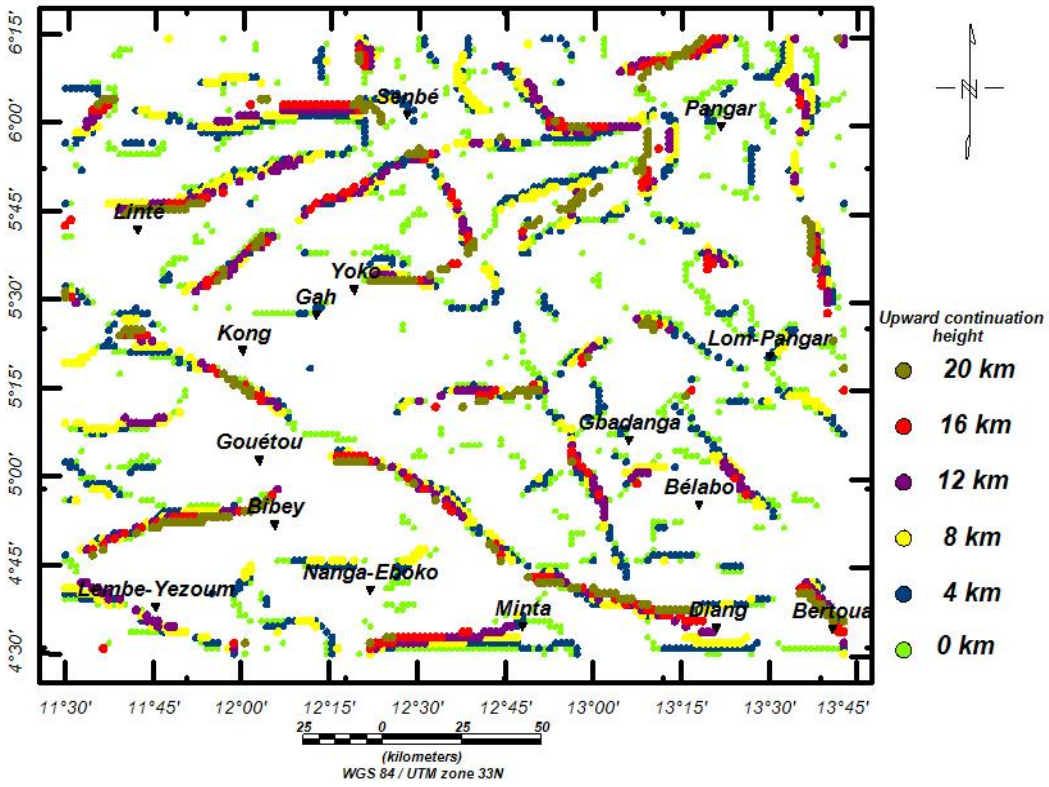

Figure 9: Map of HGMVD Extended Upwards at Different Heights

3.5. Euler Deconvolution

Based on the homogeneity equation, Euler-3D deconvolution is another geophysical filter that can characterise soil and subsoil structures [34, 35]. This process is specific in the sense that it provides information on the depth of gravity sources as well as their geographical position. The Euler deconvolution method has been applied to densify Bouguer anomalies. Considering the geographical specificities of the Lom389 Pangar region, the following combinations were applied to the area: Structural Index SI [0, 0.1, 1, and 2], window cell W [5×5, 8×8, 10 × 10, and 15 × 15], and Tolerance T [5%, 8%, 10%, and 15%].

The best combination bringing out the basement contacts or faults is: SI = 0:1, W=15, and T=15. Figure 10 shows the most efficient structural solutions obtained for the selected combination It can be seen that the study area is affected by a system of lineaments ranging from near-surface to more than 18 km depth. On the one hand, the gravity field sources do not have a uniform distribution at the scale of the map; on the other hand, major lineaments are clearly identified. The non-uniformity of the depths of the main structural signatures identified indicates that not all crustal contours have the same origin. These solutions evolve in the main directions ENE-WSW and NE-SW. On the Euler solution map, the limits of some intrusive bodies, as well as a network of faults could be highlighted.

The ENE-WSW trending Central Cameroon Shear Zone [CCSZ], which crosses the study area, is identified to the north of Linté with a vertical extension of around 15km. Intense contacts again recorded to the south, trending WNW-ESE and ENE-WSW, would probably mark the extension of the Lom Basin boundaries to which the Lom-Pangar area would belong. The maps of the local maxima of the gDHDV field calculated at different altitudes associated with the Euler417 3D deconvolution [figures 9 and 10] have helped to construct a synthetic structural map [figure 11] emphasizing the faults [F1 to F42]. The directions of the identified lineaments are given in Table 1. The rosette of directions [Figure 12] shows several groups of which the main directions are:

• those constituted by the N0-45°E directions, corresponding to that of the Cameroon Volcanic Line [CVL] or the Central Cameroon Shear Zone [CCSZ];

• Those with directions N45-90°E corresponding either as the Sanaga Shear Zone [SSZ] alignment and
• the N90-180E orientation could be due to the emplacement of the Pan-African nappe or they are the result of senestial and dexter radiation representing fractures with or without vein flow [20, 15].

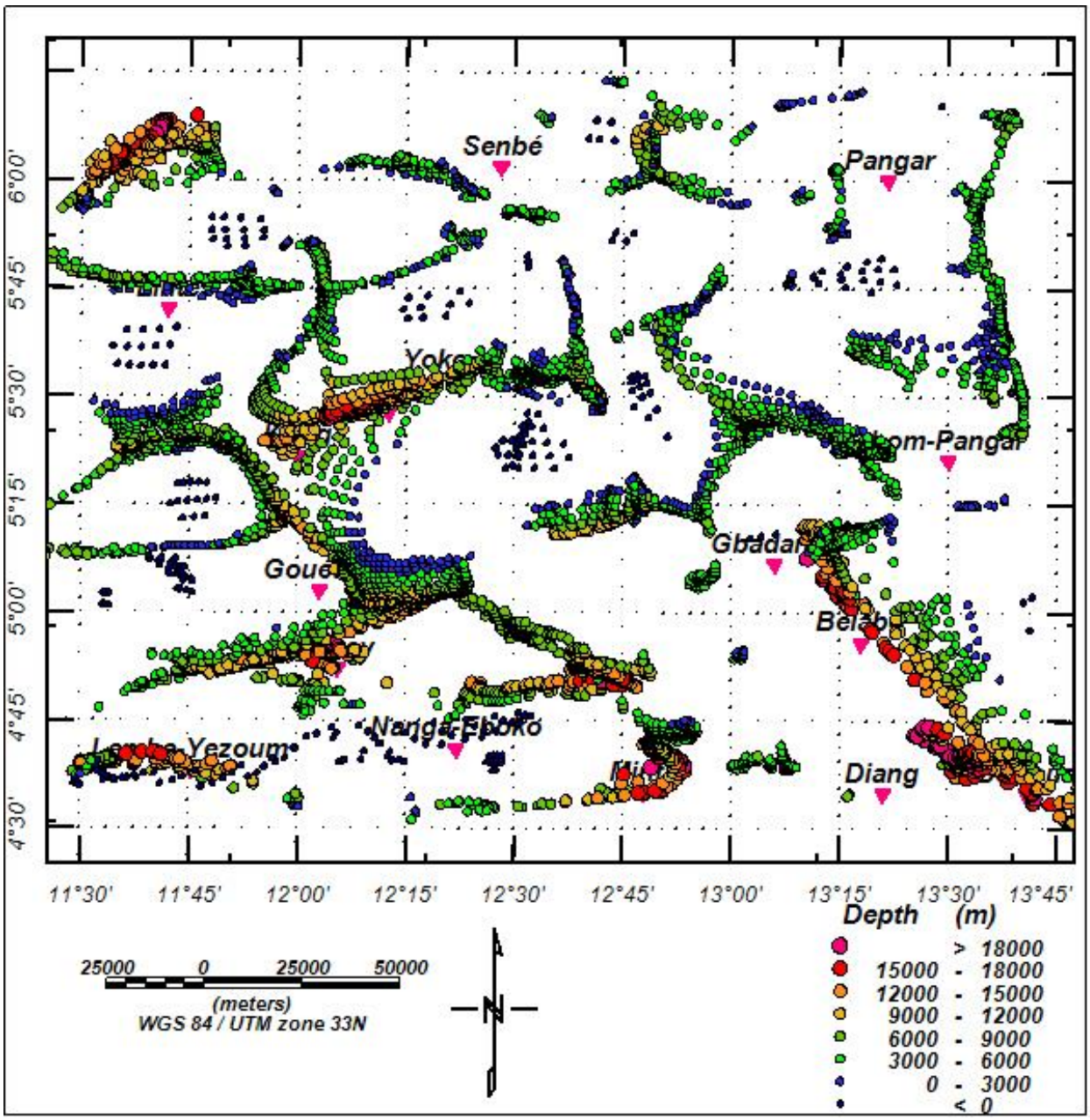

Figure 10: Euler deconvolution map a strucural index of 0.1

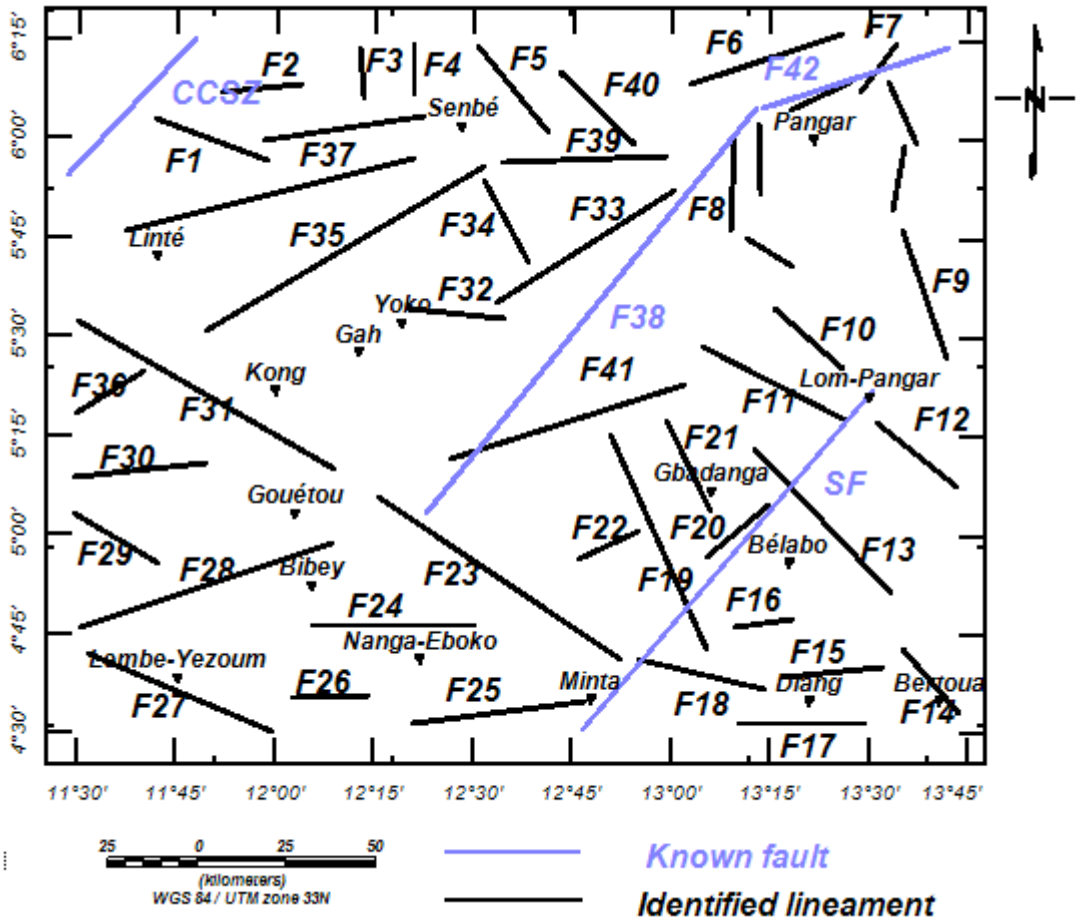

Figure 11: Structural Map of the Study Area Deduced from ANN-Densified Bouguer Anomalies

Fault	*Direction*	*Fault*	*Direction*	*Fault*	*Direction*	*Fault*	*Direction*
F1	**N 111° E**	**F12**	**N 128° E**	**F23**	**N 124° E**	**F34**	**N 151° E**
F2	**N 84° E**	**F13**	**N 138° E**	**F24**	**N 89° E**	**F35**	**N 58° E**
F3	**N 176° E**	**F14**	**N 137° E**	**F25**	**N 82° E**	**F36**	**N 53° E**
F4	**N 176° E**	**F15**	**N 84° E**	**F26**	**N 87° E**	**F37**	**N 77° E**
F5	**N 141° E**	**F16**	**N 79° E**	**F27**	**N 112° E**	**F38**	**N 39° E**
F6	**N 72° E**	**F17**	**N 88° E**	**F28**	**N 72° E**	**F39**	**N 89° E**
F7	**N 34° E**	**F18**	**N 105° E**	**F29**	**N 122° E**	**F40**	**N 46° E**
F8	**N 1° E**	**F19**	**N 156° E**	**F30**	**N 83° E**	**F41**	**N 74° E**
F9	**N 18° E**	**F20**	**N 48° E**	**F31**	**N 120° E**	**F42**	**N 72° E**
F10	**N 133° E**	**F21**	**N 151° E**	**F32**	**N 97° E**	**CCSZ**	**N 42° E**
F11	**N 118° E**	**F22**	**N 65° E**	**F33**	**N 58° E**	**SSZ**	**N 41° E**

Figure 12: Rosette of Fracture Directions Deduced from Gravity Anomalies

3.6. Local Scale

Statistical and visual analysis of the lineament map revealed three main families of orientation at the local scale [ENE-WSW, NW-SE, and NE-SW]. The central ENE-WSW direction, the most important corresponds to a serie of intense shears accompanied by mantle uplift and granitisation; it represents the normal orientation of the faults in East Cameroon. It is related to the direction of subduction of the southern part of the craton under the Adamaoua plate as well as other important faults in Cameroon such as the Sanaga Fault, the Foumban Fault, etc [20, 15].

A major part of the lineaments of this family is related to the Pan-African tectonics, the central major lineaments can be associated to the Eburnian tectonics. The NW-SE trending lineaments located mostly in the east and centre of the region reflect a subhorizontal direction of extension of the granitic magma during its emplacement once the ascent of the magma ended in the Archean. The main geological formations encountered are late syntectonic and ancient granites. The confrontation with geological field data allows linking the appearance of faults to two types of geological phenomena. (1) Plutonism phenomena including the contact between schist-granites are accentuated in our study area. (2) Tectonic features such as faults are much more pronounced in the central and northwestern parts of our region. Therefore, long lineaments correlate with geological faults in the region [36].

3.7. Regional Scale

Regionally, the study area consists of Pan-African age terrains. The tecto-metamorphic evolution here is polyphase with two successive deformations. The dextral and senestial faults, identified and all parallel to the main foliation, provide information on the late process of structural evolution. About 44 linear elements have been counted, mainly faults and lithological contacts. These linear features are grouped into three main families in proportions: N0-45°E or NE-SW [27%], N45-90°E or ENE-WSW [36%], and N90-180°E or NW-SE [37%].

Looking at these results, the influences of the structure on the geology of the region can easily be noticed. After the Archean orogeny, this region was subject to several tectonic and orogenic episodes, extensive granitisation, and metamorphism during geological time. The regional metamorphism is Pan-African in age, low pressure, and associated with transpressive tectonics; it is associated with extensive crustal melting that produced "S" type granitoid]. These faults are chronologically oriented NE-SW, WNW-ESE, and ENE460 WSW, and are likely to range in age from Archean to Pan-African; their presence also justifies the intermediate character of the Pan-African Range, which lies between the N-S oriented Trans-Saharan Ranges and the E-W oriented Oubanguid Range [37].

4. Discussion

4.1. Validation of Results

This study is based in the Lom-Pangar region; an area belonging to the volcano-sedimentary basin of the Lom series. From the geological identities newly located and the recovered old ones, the set of recorded results justifies the reliability of the densified gravity data by the artificial neural method [ANN] previously presented in the works of [5, 38]. According to authors such as land gravity data remain one of the best tools for studying the subsoil or the earth's crust. As the present in-situ gravity data are from poor resolution, the particularly revolutionary interpolation technique used here [ANN] has made it possible to optimise the gravity coverage of the region while at the same time alleviating the problem of low data density and their sparse nature [25, 30, 39, 40].

The study area includes sedimentary basins, a basement that is believed to be granite-gneissic, with upwelling of dense material from the upper mantle, and multiple faults [CCSZ and SSZ] initially highlighted by; it therefore presents a real challenge for a thorough structural investigation. The densified gravity data following the artificial neural network effectively highlights the geophysical response of the geology in the study area [4]. The continuous upward maps highlighted a regional structure-oriented NE-SW to the NE and W-E to the south in line with the work of [20, 27]. The three sets characterized in the field [NE-SW, NW-SE, and ENE-WSW] all belong to the Pan-African domain and correspond well to three geological domains of different age and evolution namely the syn-tectonic granites in the east, the Lom series in the center and the metamorphic series in the northwest.

The ENE-WSW orientation is indeed the one that characterizes the Pan-African tectonics at the regional scale, it has been highlighted in the Adamaoua structures that cover part of the study area, by [12, 27]. This is also the direction of the major Pan-African structures in Cameroon, namely the Central Cameroon Shear and the Sanaga Fault, while the WNW-ESE orientation is due to the emplacement of the Pan-African nappe, i.e. a senestial and dexterous radiation representing fractures with or without vein flow [20, 15. The major tectonic lines mapped are locally linked to: (1) the ENE-WSW oriented deep fault network which could extend to Betare-Oya; (2) the NW-SE oriented deep collapse faults with lowered compartments for the tectonic lines of the same orientation. On a regional scale, their origin is associated to two main sets of folds and brittle tectonic lines with the collision between the southern Congo Craton plate and the northern Adamaoua plate.

Interpretation of the gravity data in the study area revealed the presence of faults. The different orientations of these faults imply that the region has undergone several tectonic events. This information on the orientation of the surface and deep faults, and intrusive structures can be used to determine the direction of fluid flow within the sedimentary cover and the presence of potential mineral deposits, given that the entire East Cameroon region has real mining potential. The artificial neural network is therefore suitable for geophysical investigation considering the density variability of the subsurface structure. Moreover, the maxima of the horizontal gradient of the vertical derivative recorded at different altitudes, coupled with the Euler-3D solutions, allow to characterise the essential lineament characteristics of the region. The latter two techniques have feature depth limits of around 20 km.

4.2. Structural Contribution

The first contribution of this work is methodological. Indeed, following the work done by, and in the light of the geophysical results obtained in this work, geophysics is now enriched by a new data interpolation technique. Work in and around the Lom-Pangar area has highlighted lineaments as associated with faults and contacts, using geological, gravity and aeromagnetic surveys [4, 5, 36, 41, 42]. Field geopotential data, in particular densified gravity data following the ANN (Diffo et al., 2022) [5] Considering the results of this study, they allow to identify some very deep structures considering the rather small size of our study area, according to the density variations of the geological structures present at the level of the earth crust.

Figure 10 shows the major lineaments resulting from the combination of the different geophysical processing methods used in this study [maxima of the horizontal gradient of the vertical derivative coupled with Euler solutions]. This figure 10 highlights the well-known old lineaments in the area and reveals new ones. The characterisation of the known lineaments attests to the effectiveness of the neural architecture model validated for this study in highlighting linear features in the subsurface interpreted as faults or geological contacts. Thus, a synoptic table [Table 1] summarizes the directions of the main lineaments by previous work. Although the area of investigation was quite small and the data set very sparse, the densification has allow obtaining more than forty lineaments in the area. Known faults are depicted with considerable vertical extensions [nearly 20km], notably the faults of the Central Cameroon Shear Zone [CCSZ] or the Sanaga Shear Zone [SSZ] [43-57].

The multitude of lineament directions obtained together with their vertical extension is indicative of the quality of the dataset used. The statistical analysis is shown by the directional rosette [Figure 11] comprising the confirmed and revealed lineaments. It largely reflects the CCSZ and SSZ directions as the main tectonic features of the NE523 SW oriented study area. This new approach [ANN], having brought out new lineaments, combined with the previous ones, would allow us to qualify the study area as highly fractured. These interesting findings underline a certain interest in future research not only in the Lom-Pangar region but also in the interpolation technique used [ANN]. As well, they help to validate the neural approach used in this work. However, for more diversity in the results obtained in the area, this neural approach could be combined with other investigative techniques such as seismic, aeromagnetic, satellite imagery, or geological soil prospection.

5. Conclusion

The study examined the structural characteristics of the Lom-Pangar region in East Cameroon using Bouguer anomalies obtained in-situ and then densified by the artificial neural network [ANN] method. Densified gravity data filtering using the ANN method is effective in exploring the study area. The NE-SW and NW-SE directions are the main structural features revealed as confirmed by the pink diagram. Furthermore, the ENE-WSW orientation appears to be the main direction of the major Pan-African structures in Cameroon, namely the Central Cameroon Shear and the Sanaga Fault; as opposed to WNW-ESE which would be due to the emplacement of the Pan-African nappe.

The different orientations of the faults imply that the study area has undergone several tectonic events; their depths and the presence of intrusive structures can help determine the direction of fluid flow but also the presence of potential mineral deposits within the sedimentary cover. It was thus possible to note a certain concordance between the geological formations such as the identified sedimentary basins and the gravimetric anomalies densified according to the neural approach. New lineamentary structures have been identified in the area. These faults were identified as both lateral and vertical extensions of the Sanaga Shear Zone [SSZ] or the Cameroon Volcanic Line [CVL]. This work corroborates once again with the tectonic and geological complexity of the Lom-Pangar region. Acknowledgements The authors are indebted to the IRD [Institute de Recherche pour le Development] for providing the data used in this work. Compliance with ethical standards Conflict of interest on behalf of all authors, the corresponding author states that there is no conflict of interest.

References

1. Vicat, J. P., & Bilong, P. (1998). Esquisse géologique du Cameroun. Géosciences au Cameroun, 1, 3-11.
2. Gazel, J. & G. Gérard (1954) Carte géologique de reconnaissance du cameroun au 1/500 000, feuille Batouri-Est 587 avec notice explicative. Memoir. Direction Mines Géologie, Yaoundé Cameroun.
3. Kankeu, B. (2008). Anisotropie de la susceptibilité magnétique (ASM) et fabriques des roches Néoprotérozoiques des régions de Garga-Sarali et Bétaré-Oya à l'Est Cameroon: implications géodynamiques pour l'évolution de la chaîne panafricaine d'Afrique Centrale (Doctoral dissertation, Ph. D. thesis. Université de Yaoundé I).
4. Toteu, S. F., Penaye, J., Deschamps, Y., Maldan, F., Nyama Atibagoua, et al. (2008, August). Géologie et ressources minérales du Cameroun. In 33rd International Geological Congress, Oslo, Norway.
5. Diffo, S., Lemotio, W., Mezoue Adiang, C., Ngatchou Heutchi, E., Nguiya, S., et al. (2022). Contribution of the artificial neural network (ANN) method to the interpolation of the Bouguer gravity anomalies in the region of Lom-Pangar (East-Cameroon). Geomechanics and Geophysics for Geo-Energy and Geo-Resources, 8(1), 32.
6. Fon, A. N., Che, V. B., & Suh, C. E. (2012). Application of electrical resistivity and chargeability data on a GIS platform in delineating auriferous structures in a deeply weathered lateritic terrain, eastern Cameroon. International Journal of Geosciences, 3(05), 960.
7. Cornacchia, MAURICE, & Dars, REN É. (1983). A major structural feature of the African continent; the Central African lineaments from Cameroon to the Gulf of Aden. Bulletin of the Geological Society of France, 7 (1), 101-109.
8. Ngako, F., Jegouzo, P., & Nzenti, J. P. (1991). Le Cisaillement Centre Camerounais. Rôle structural et géodynamique dans l'orogenèse panafricaine. Comptes rendus de l'Académie des sciences. Série 2, Mécanique, Physique,

Chimie, Sciences de l'univers, Sciences de la Terre, 313(4), 457-463.
9. Mvondo, H., Den Brok, S. W. J., & Ondoa, J. M. (2003). Evidence for symmetric extension and exhumation of the Yaounde nappe (Pan-African fold belt, Cameroon). Journal of African Earth Sciences, 36(3), 215-231.
10. Mvondo, H., Owona, S., Ondoa, J. M., & Essono, J. (2007). Tectonic evolution of the Yaoundé segment of the Neoproterozoic Central African Orogenic Belt in southern Cameroon. Canadian Journal of Earth Sciences, 44(4), 433-444.
11. Olinga, J. B., Mpesse, J. E., Minyem, D., Ngako, V., Mbarga, T. N., et al. (2010). The Awae Ayos strike-slip shear zones (southern Cameroon): Geometry, kinematics and significance in the late Pan-African tectonics. Neues Jahrbuch für Geologie und Paläontologie-Abhandlungen, 1-11.
12. Feumoe, A. N. S., Ndougsa-Mbarga, T., Manguelle-Dicoum, E., & Fairhead, J. D. (2012). Delineation of tectonic lineaments using aeromagnetic data for the south-east Cameroon area. G eofizika, 29(2), 175-192.
13. Njonfang, E., Ngako, V., Moreau, C., Affaton, P., & Diot, H. (2008). Restraining bends in high temperature shear zones: the "Central Cameroon Shear Zone", Central Africa. Journal of African Earth Sciences, 52(1-2), 9-20.
14. Ngalamo, J. F. G., Sobh, M., Bisso, D., Abdelsalam, M. G., Atekwana, E., et al. (2018). Lithospheric structure beneath the Central Africa Orogenic Belt in Cameroon from the analysis of satellite gravity and passive seismic data. Tectonophysics, 745, 326-337.
15. Kankeu, B., Greiling, R. O., & Nzenti, J. P. (2009). Pan-African strike–slip tectonics in eastern Cameroon—Magnetic fabrics (AMS) and structure in the Lom basin and its gneissic basement. Precambrian Research, 174(3-4), 258-272.
16. Hamdi Nasr, I., Amiri, A., Hédi Inoubli, M., Ben Salem, A., Chaqui, A., et al. (2011). Structural setting of northern Tunisia insights from gravity data analysis Jendouba case study. Pure and Applied Geophysics, 168, 1835-1849.
17. Koumetio, F., Njomo, D., Tatchum, C. N., Tokam, A. P. K., Tabod, T. C., et al. (2014). Interpretation of gravity anomalies by multi-scale evaluation of maxima of gradients and 3D modelling in Bipindi region (South-West Cameroon). International journal of Geosciences, 5(12), 1415.
18. Poudjom Djomani, Y. H., & Diament, M. (1992). Modélisation 2-D d'un profil gravimétrique au Cameroun. Stage de fin de première année de Magistère IPGP.
19. Tadjou, J. M. (2004). Apport de la gravimétrie à l'investigation géophysique de la bordure septentrionale de Craton du Congo (Sud-Cameroun) (Doctoral dissertation, Thése de Doctorat/Ph. D, Univ. Yaoundé I, 178 pages).
20. Nguiya, S. (2009). Investigation géophysique du bassin volcano-sédimentaire de Lom (Est-Cameroun): Implications structurale et recontinued (Doctoral dissertation, Thèse de Doctorat/PhD Université de Yaoundé I).
21. Dorbath, C. 1984. Approche sismologique de la structure de la lithosphere en Afrique de l'Ouest.
22. Dorbath, L. & C. Dorbath. 1984. Approche Sismologique de la Lithosphère en Afrique de l'Ouest. Thèse de Doctorat, Université Pierre et Marie Curie, Paris.
23. Stuart, G. W., Fairhead, J. D., Dorbath, L., & Dorbath, C. (1985). A seismic refraction study of the crustal structure associated with the Adamawa Plateau and Garoua Rift, Cameroon, West Africa. Geophysical Journal International, 81(1), 1-12.
24. Tokam, A. P. K., Tabod, C. T., Nyblade, A. A., Julia, J., Wiens, D. A., & Pasyanos, M. E. (2010). Structure of the crust beneath Cameroon, West Africa, from the joint inversion of Rayleigh wave group velocities and receiver functions. Geophysical Journal International, 183(2), 1061-1076.
25. Poudjom, DYH (1993). Contribution of Gravimetry to the study of the continental Lithosphere and geodynamic implications. Study of an intraplate bulge: The Adamaoua massif (Cameroon). University of Paris-Sud (unpublished).
26. Jacobsen, B. H. (1987). A case for upward continuation as a standard separation filter for potential-field maps. Geophysics, 52(8), 1138-1148.
27. Noutchogwe, C. T., Koumetio, F., & Manguelle-Dicoum, E. (2010). Structural features of South-Adamawa (Cameroon) inferred from magnetic anomalies: Hydrogeological implications. Comptes Rendus Geoscience, 342(6), 467-474.
28. Toteu, S. F., Penaye, J., & Djomani, Y. P. (2004). Geodynamic evolution of the Pan-African belt in central Africa with special reference to Cameroon. Canadian Journal of Earth Sciences, 41(1), 73-85.
29. Jaffal, M., El Goumi, N., Kchikach, A., Aïfa, T., Khattach, D., et al. (2010). Gravity and magnetic investigations in the Haouz basin, Morocco. Interpretation and mining implications. Journal of African Earth Sciences, 58(2), 331-340.
30. Hadhemi, B., Fatma, H., Ali, K., & Mohamed, G. (2016). Subsurface structure of Teboursouk and El Krib plains (dome zone, northern Tunisia) by gravity analysis. Journal of African Earth Sciences, 119, 78-93.
31. Cordell, L., & Grauch, V. J. S. (1985). Mapping basement magnetization zones from aeromagnetic data in the San Juan Basin, New Mexico. In The utility of regional gravity and magnetic anomaly maps (pp. 181-197). Society of Exploration Geophysicists.
32. Fotze, Q. M. A., Basseka, C. A., Lordon, A. E. D., Yomba, A. E., Shandini, Y., et al. (2019). Geophysical Data Processing for the Delineation of Tectonic Lineaments in South Cameroon. Earth Science Research, 8(2), 1-1.
33. Koumetio, F., Njomo, D., Tabod, C. T., Noutchogwe, T. C., & Manguelle-Dicoum, E. (2012). Structural interpretation of gravity anomalies from the Kribi–Edea zone, South Cameroon: a case study. Journal of Geophysics and Engineering, 9(6), 664-673.
34. Thompson, D. T. (1982). EULDPH: A new technique for making computer-assisted depth estimates from magnetic data. Geophysics, 47(1), 31-37.
35. Keating, M. (1998). The new regionalism in Western Europe: territorial restructuring and political change. Cheltenham, UK: E. Elgar.
36. Cheunteu Fantah, C. A., Mezoue, C. A., Mouzong, M. P., Tokam Kamga, A. P., Nouayou, R., & Nguiya, S. (2022). Mapping of major tectonic lineaments across Cameroon using potential field data. Earth, Planets and Space, 74(1), 1-19.

37. Meying, A., Ndougsa-Mbarga, T., & Manguelle-Dicoum, E. (2009). Evidence of fractures from the image of the subsurface in the Akonolinga-Ayos area (Cameroon) by combining the Classical and the Bostick approaches in the interpretation of audio-magnetotelluric data. Journal of Geology and Mining Research, 1(8), 159-171.
38. Mouzong Pemi, M., Kamguia, J., Nguiya, S., & Manguelle-Dicoum, E. (2018). Depth and lineament maps derived from North Cameroon gravity data computed by artificial neural network. International Journal of Geophysics, 2018.
39. Nasr, I. H., Salem, A. B., Inoubli, M. H., Dhifi, J., Alouani, R., et al. (2008). Apports de la gravimétrie dans la caractérisation des structures effondrées dans la région de Nebeur (Nord Ouest de la Tunisie). Swiss Journal of Geosciences, 101, 17-27.
40. Hamdi-Nasr, I., Inoubli, M. H., Salem, A. B., Tlig, S., & Mansouri, A. (2009). Gravity contributions to the understanding of salt tectonics from the Jebel Cheid area (dome zone, Northern Tunisia). Geophysical Prospecting, 57(4), 719-728.
41. Ngako, V., Njonfang, E., Aka, F. T., Affaton, P., & Nnange, J. M. (2006). The North–South Paleozoic to Quaternary trend of alkaline magmatism from Niger–Nigeria to Cameroon: complex interaction between hotspots and Precambrian faults. Journal of African Earth Sciences, 45(3), 241-256.
42. Ngako, V., Njonfang, E., Aka, F. T., Affaton, P., & Nnange, J. M. (2006). The North–South Paleozoic to Quaternary trend of alkaline magmatism from Niger–Nigeria to Cameroon: complex interaction between hotspots and Precambrian faults. Journal of African Earth Sciences, 45(3), 241-256.
43. Biyiha-Kelaba, W., Ndougsa-Mbarga, T., Yene-Atangana, J. Q., Ngoumou, P. C., & Tabod, T. C. (2013). 2.5 D Models derived from the magnetic anomalies obtained by upwards continuation in the Mimbi area, southern Cameroon. Journal of earth sciences and Geotechnical Engineering, 3(4), 175-199.
44. Blakely, R. J., & Simpson, R. W. (1986). Approximating edges of source bodies from magnetic or gravity anomalies. Geophysics, 51(7), 1494-1498.
45. Claude, N. P., Patrick, A. S., Igor, O. A. O. U., Arsene, M., Justine, Y., et al. (2021). 2.5 D Crustal models derived from analytical polynomial separation technique and spectral analysis of gravity data with their probable gold mineralization migrations (Batouri, SE-Cameroon).
46. Abate Essi, J. M., Marcel, J., Yene Atangana, J. Q., Ahmad, A. D., Fita Dassou, E., et al. (2017). Interpretation of gravity data derived from the Earth Gravitational Model EGM2008 in the Center-North Cameroon: structural and mining implications. Arabian Journal of Geosciences, 10, 1-13.
47. Grauch, V. J. S., & Cordell, L. (1987). Limitations of determining density or magnetic boundaries from the horizontal gradient of gravity or pseudogravity data. Geophysics, 52(1), 118-121.
48. Marcel, C. J., Tabor, E., & Njandjock, P. N. (2019). Moho discontinuity depth estimates for the Cameroon Volcanic Line from gravity data. International Journal of Economic and Environmental Geology, 17-20.
49. Marcel, J., Abate Essi, J. M., Nouck, P. N., Sanda, O., & Manguelle-Dicoum, E. (2018). Validation of gravity data from the geopotential field model for subsurface investigation of the Cameroon Volcanic Line (Western Africa). Earth, Planets and Space, 70(1), 1-18.
50. Marson, I., & Klingele, E. E. (1993). Advantages of using the vertical gradient of gravity for 3-D interpretation. Geophysics, 58(11), 1588-1595.
51. Ndougsa-Mbarga, T., Meying, A., Bisso, D., Sharma, K. K., Layu, D. Y., & Manguelle-Dicoum, E. (2011). Audiomagnetotellurics (AMT) soundings based on the Bostick approach and evidence of tectonic features along the northern edge of the Congo Craton, in the Messamena/Abong-Mbang area (Cameroon). Journal of Indian Geophysical Union, 15(3), 145-159.
52. Noutchogwe, T. C. (2010). Investigation géophysique dans la région de l'Adamaoua par les méthodes gravimétriques et magnétiques: implications structurales et hydrogéologiques. Yaounde: Université de Yaoundé I.
53. Nguimbous-Kouoh, J. J., Ngos III, S., Mbarga, T. N., & Manguelle-Dicoum, E. (2017). Use of the Polynomial Separation and the Gravity Spectral Analysis to Estimate the Depth of the Northern Logone Birni Sedimentary Basin (CAMEROON). International Journal of Geosciences, 8(12), 1442-1456.
54. Reid, A., FitzGerald, D., & Flanagan, G. (2005, November). Hybrid Euler magnetic basement depth estimation: Bishop 3D tests. In SEG International Exposition and Annual Meeting (pp. SEG-2005). SEG.
55. Reid, A. B., Allsop, J. M., Granser, H., Millett, A. T., & Somerton, I. W. (1990). Magnetic interpretation in three dimensions using Euler deconvolution. Geophysics, 55(1), 80-91.
56. Soba, D. (1989). La série du Lom: étude géologique et géochronologique d'un bassin volcano-sédimentaire de la chaine panafricaine à l'Est du Cameroun (Doctoral dissertation, Paris 6).
57. Toteu, S. F., Van Schmus, W. R., Penaye, J., & Michard, A. (2001). New U–Pb and Sm–Nd data from north-central Cameroon and its bearing on the pre-Pan African history of central Africa. Precambrian Research, 108(1-2), 45-73.